

NASA Technical Memorandum 107149

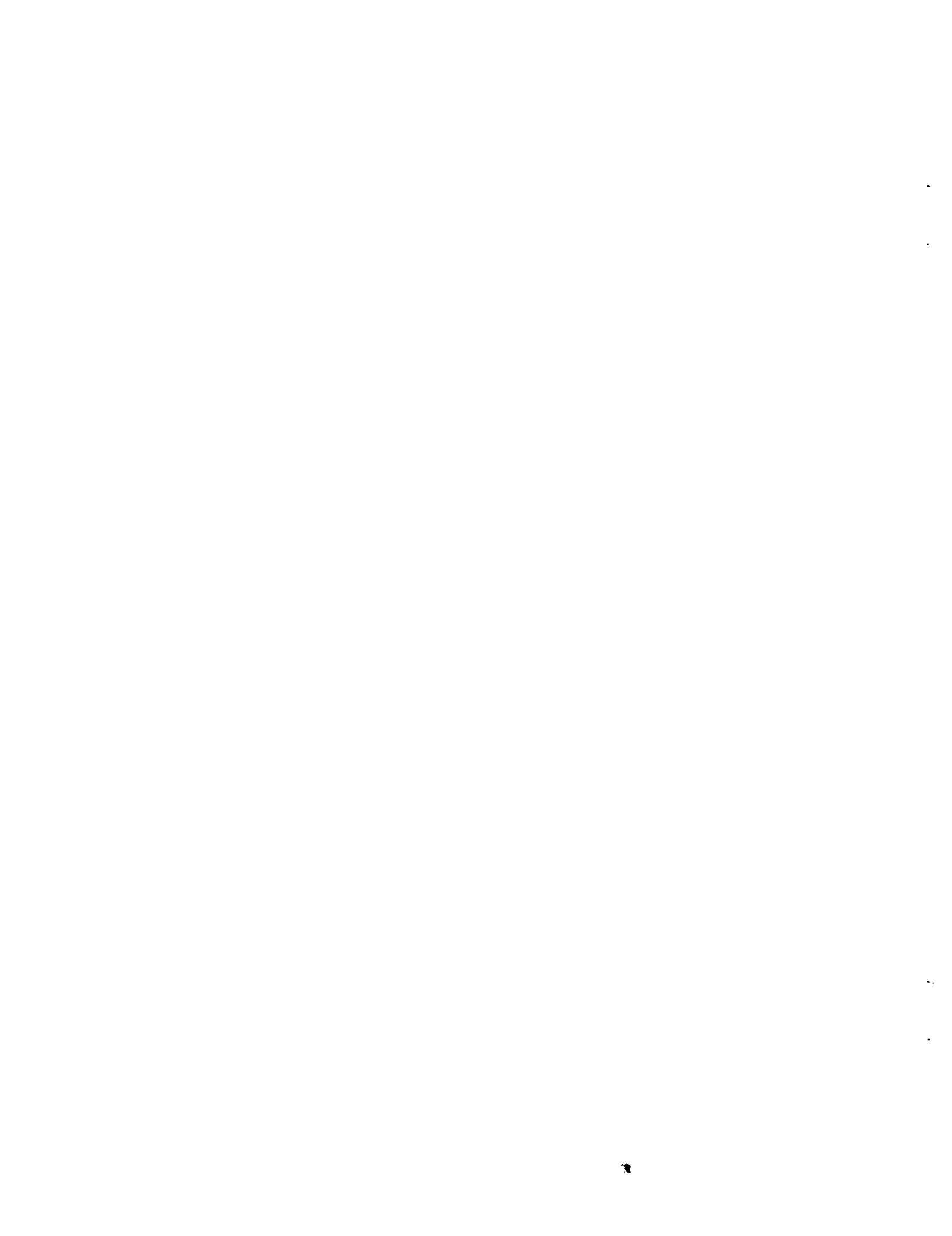
A Self Calibrating Emissivity and/or Transmissivity Independent Multi- wavelength Pyrometer

Daniel Ng
Lewis Research Center
Cleveland, Ohio

January 1996



National Aeronautics and
Space Administration



A SELF CALIBRATING EMISSIVITY AND/OR TRANSMISSIVITY INDEPENDENT MULTIWAVELENGTH PYROMETER

DANIEL NG
NASA Lewis Research Center
Cleveland, OH 44135

Introduction

Pyrometer is a favorite method to do remote temperature measurement in research and development. One-color, two-color and the disappearing filament pyrometers⁽¹⁾ are most common, multicolor and multiwavelength pyrometers are being introduced recently⁽²⁻⁴⁾. All these pyrometers invariably require, in one form or another, information concerning emissivity, the medium transmissivity, their ratio at some two spectral regions, the instrument's calibration constant, etc. for their operation. This information can come from hand books, from the manufacturer or in some instances, from results of dedicated separate experiments. Often this information is sample or instrument specific. Sometimes this information, though obtained from a special experiment, is obtained using a separate sample rather than the one pursued for temperature measurement. Then, there would be the question of variability from sample to sample and variability from batch to batch in the sample used. Also, previously determined calibrations can change with time, and the only way to reduce uncertainty is to perform the calibration more frequently or even immediately before the experiment. We have developed a multiwavelength pyrometer, which eliminates the need to supply the necessary emissivity and/or transmissivity information and the instrument calibration constants ahead of time. The pyrometer calibrates itself from its first cycle data.

Theory

Planck's law of black body radiation (Eqn 1) is the foundation of pyrometry, with c_1 , c_2 the radiation constants, λ the wavelength and T the black body temperature.

$$L(\lambda, T) = \frac{c_1}{\lambda^5} \frac{1}{\exp(c_2/\lambda T) - 1} \quad (1)$$

In its most basic form, a pyrometer is a spectrometer which records a voltage $V(\lambda, t)$ at time t in response to radiation emitting from a black body. In general, the radiation source is not a black body, and the output voltage $V(\lambda, t)$ depends on ϵ_λ , the spectral emissivity of the emitting body, τ_λ the transmissivity of the optical medium between the emitting body and the detector, and the instrument constant g_λ given by Eqn 2

$$V(\lambda, T(t)) = g_\lambda \epsilon_\lambda \tau_\lambda \frac{c_1}{\lambda^5} \frac{1}{\exp(c_2/\lambda T(t)) - 1} \quad (2)$$

The temperature is assumed to be a function of t . Ideally, if g , ϵ and τ are known at wavelength λ , temperature measurement is reduced to measurement of $V(\lambda, T)$ only. In general, g , ϵ and τ are not known. We show that though temperatures $T(t_1) \neq T(t_2) \neq \dots \neq T(t_n)$ are unknown, spectra of wavelengths $\lambda_1, \lambda_2, \dots, \lambda_N$, $N > 2$, obtained at times t_1, t_2, \dots, t_n , contain enough information to determine everything that is required in pyrometry. Consider at time t , 2 wavelengths, label them and their associated quantities by λ_R and λ_i

$$V(\lambda_R, t) = g_{\lambda_R} \epsilon_{\lambda_R} \tau_{\lambda_R} \frac{c_1}{\lambda_R^5} \frac{1}{\exp(c_2/\lambda_R T(t)) - 1} \quad (3)$$

$$V(\lambda_i, t) = g_{\lambda_i} \epsilon_{\lambda_i} \tau_{\lambda_i} \frac{c_1}{\lambda_i^5} \frac{1}{\exp(c_2/\lambda_i T(t)) - 1} \quad (4)$$

Solve for $T(t)$, replace subscripts λ_R, λ_i by just R and i in g, ϵ and τ , we have

$$T(t) = \frac{c_2/\lambda_R}{\text{Log}_e \left(g_R \epsilon_R \tau_R \frac{c_1}{\lambda_R^5} \frac{1}{V(\lambda_R, t)} + 1 \right)} = \frac{c_2/\lambda_i}{\text{Log}_e \left(g_i \epsilon_i \tau_i \frac{c_1}{\lambda_i^5} \frac{1}{V(\lambda_i, t)} + 1 \right)} \quad (5)$$

$$\frac{c_1}{\lambda_i^5} \frac{1}{V(\lambda_i, t)} = \frac{1}{g_i \epsilon_i \tau_i} \left\{ \left(g_R \epsilon_R \tau_R \frac{c_1}{\lambda_R^5} \frac{1}{V(\lambda_R, t)} + 1 \right)^{\frac{\lambda_R}{\lambda_i}} - \frac{1}{g_i \epsilon_i \tau_i} \right\} \quad (6)$$

Eliminating temperature $T(t)$ yields Eqn 6 from Eqn 5. Letting $A_R = g_R \epsilon_R \tau_R$ and $A_i = g_i \epsilon_i \tau_i$, Eqn 6 becomes Eqn 7, this is the equation which we will use.

$$\frac{c_1}{\lambda_i^5} \frac{1}{V(\lambda_i, t)} = \frac{1}{A_i} \left\{ \left(A_R \frac{c_1}{\lambda_R^5} \frac{1}{V(\lambda_R, t)} + 1 \right)^{\frac{\lambda_R}{\lambda_i}} - \frac{1}{A_i} \right\} \quad (7)$$

Assume $A_R = g_R \epsilon_R \tau_R$ is constant, i.e. time and temperature independent, the $A_i = g_i \epsilon_i \tau_i$ may dependent on temperature, then a plot of the quantity on the left hand side vs the quantity inside the curly brackets on the right hand side of Eqn 7 will produce a straight line of slope $1/A_i = 1/g_i \epsilon_i \tau_i$ and intercept $-1/A_i = -1/g_i \epsilon_i \tau_i$. Do this for all $i \neq R$. The spectral quantity A_i is a function of A_R . Referring to Eqn 5 or its equivalent, Eqn 8, use the generated A_i to calculate the temperature $T(\lambda, t)$ at time t .

$$T(\lambda, t) = \frac{c_2/\lambda_i}{\text{Log}_e \left(A_i \frac{c_1}{\lambda_i^5} \frac{1}{V(\lambda_i, t)} + 1 \right)} \quad (8)$$

In theory, these calculated temperatures should all equal to each other and be independent of wavelength. In actual data, there are variations, an average $T(t)$ is obtained according to Eqn. 9.

$$T(t) = \frac{\sum_1^N T(\lambda, t)}{N} \quad (9)$$

This is done for all the spectra (i.e all t) to obtain average temperatures as determined by a particular value of A_R . The correct value A_R is determined by a least squares procedure as follows:

- 1) Choose a value for A_R .
- 2) Plot the data according to Eqn 7 to determine the A_i from the slopes.
- 3) Use the so determined A_i to calculate the temperatures $T(t)$ according to Eqns. 8 & 9.
- 4) Transform the spectra $V(\lambda_i, t)$ into a large data set (x, y) . The wavelength λ_i is transformed into $c_2/\lambda T(t)$, the transformed wavelength, the voltage $V(\lambda_i, t)$ is divided by A_i , and then by $T(t)^5$, the 5th power of the spectrum temperature, according to the prescription

$$x = \frac{c_2}{\lambda T(t)}, \quad y = \frac{V(\lambda, t)}{A} \frac{1}{T(t)^5} = \frac{c_1}{c_2^5} \frac{x^5}{e^{x-1}} \quad (10)$$

- 5) The transformed (x, y) data obey the generalized non-dimensional Planck function. The (x, y) data is fitted to the Planck function of Eqn. 10 by calculating the residual. The residual Σ , is defined as the sum of the squares of the difference between the transformed y_i and the calculated y evaluated by substituting the transformed x_i in the y equation in Eqn 10 for all the data.
- 6) A new value for A_R is selected and steps (2 to 5) repeated,
- 7) The particular value of A_R that produced the least Σ is the correct one.

Thus in one step, A_R , also A_i and $T(t)$ are determined. In one stroke, everything that is needed in

pyrometry for temperature measurement is determined. Temperatures at any time in the past or in the future are determined from each λ according to Eqn 4 or its equivalent Eqn 8. As is evident, the pyrometer requires no prior calibration. When $N=2$, A_i is defined in terms of A_R and the slope of the experimental data. The correct value of A_R is similarly determined by least squares curve fitting the $N=2$ smaller transformed (x,y) data sets at different temperatures exactly as described above to Eqn 10. Greater redundancy is achieved when $N \geq 2$.

Experiment and Results

Two sets of results are presented. The first is temperature measurement of a black body furnace viewed through a window of unknown transmissivity, the spectrometer has not been calibrated. The second one is the temperature measurement of a zirconia ceramics of unknown emissivity, the spectrometer has been calibrated.

(I) Unknown Transmissivity Case

The experimental arrangement is shown in fig. 1. This is the case of unknown g_λ , unknown τ_λ and $\epsilon_\lambda=1$. A commercial black body furnace operated between 1000 °C and 2000 °C is used. Its graphite heating element and cavity are protected against oxidation by an inert argon gas curtain. When viewing the black body cavity directly is not required, a calcium fluoride window is normally positioned at the furnace opening to reduce the argon gas consumption. In the described experiment, the calcium fluoride window was always left in place. The black body furnace temperature was increased in steps by gradually changing the controller from its lowest to its maximum temperature set point. An indicator is present to show whether the pre-set temperature has been reached. When that occurred, a spectrum was recorded. The spectrum spanned the spectral region from 0.6 to 4.5 μm . It recorded the direct voltage output of the indium antimonide detector.

Results Six of these spectra are shown in fig. 2. The spectrum minima are due to atmospheric CO_2 and H_2O absorptions in the optical path between the detector and the black body source. Following the analysis above, λ_R is chosen to be at 2 μm . An arbitrary initial value for A_R is used, plots according to Eqn 7 are made. Fig. 3 shows the case for $\lambda_R=2 \mu\text{m}$, and $\lambda_1=1.5 \mu\text{m}$, $A_R=0.1534$. It is indeed a straight line. The slope and intercepts of plots like this at other wavelengths are obtained using least squares method. They are plotted in fig. 4. Individual A_i is obtained from the slope data because less noise is present, the result is shown in fig. 5. The A_i are now used to calculate the temperature of each spectrum according to Eqn 8 and shown in fig. 6. These calculated temperatures are almost independent of wavelength. The explosion at the shortest wavelength is due to poor signal to noise there, and we excluded data at wavelength shorter than 0.8 μm in the analysis. An average is obtained for each spectrum, i.e. at time t . When the value of A_R changes, the slopes also change, hence A_i , which depend on the slopes, also change and finally the temperatures at each wavelength, calculated using A_i and the spectral data, also change. Of the many possible values that A_R can assume, we identify the correct one using the least squares curve fitting method, when the reduced (x,y) data set is used to fit the non-dimensional Planck function of Eqn 10. The least squares condition is obtained when $A_R=0.1534$ and the result is shown in fig. 7. Six spectra were used. More spectra could be used. Using more spectra would increase the (x,y) data set size, and greater redundancy, leading to better accuracy. The maximum number of spectra that we can use is limited only by computer memory. With the determination of just one parameter A_R , the A_i at all other wavelengths as well as the temperatures of all the spectra that were included in the analysis are also determined at once. Once A_i is determined, the temperature at any time in the past or in the future are determined immediately from the measured spectra. Alternately, this procedure can be repeated as often as required to update the calibration.

The measured temperatures are 2234, 2143, 1965, 1804, 1667, 1550, 1460, 1379, 1313 and 1256 K, when the black body furnace controller pre-set temperatures are 2293, 2133, 1955, 1793, 1668, 1574, 1448, 1378, 1318 and 1268 K. The results are shown in fig. 8. The agreement is within 0.5 %, except at the pre-set temperature of 2293 K, when the measured temperature is 2.5 % lower. We believe that the measured temperature is actually more correct, because during the experiment, according to the

controller indicator, the black body furnace never reached its set point temperature. The controller required a power line voltage of 220 V, but the actual line voltage is only 208 V. The temperature 2234 K was the equilibrium temperature when the controller was delivering its maximum power output under the experimental line voltage condition.

For the $N=2$ case, we choose $\lambda_R=2 \mu\text{m}$, $\lambda_I=1.5 \mu\text{m}$. With 6 spectra, there are now 12 data points in the transformed data set (x,y) . Least squares curve fitting these data to Eqn 10 gives the value 0.1471 for A_R . The fitted curve is shown in fig. 9, and the resulting temperatures for the spectra are 2262, 2169, 1987, 1822, 1683, 1564, 1472, 1390, 1323 and 1265 K, which are plotted in fig. 10. The largest error in these temperatures is less than 1.7 % of the pre-set temperatures. The use of only two wavelengths greatly reduced the data acquisition time by a factor of 10 or even 100.

(II) Unknown Emissivity Case

This is the case of unknown ϵ_λ , known g_λ and $\tau_\lambda=1$. Emission spectra of a 250 μm thick zirconia (ZrO_2) thermal barrier coating (TBC) are measured using the pyrometer arrangement of fig. 11 from 1.3 to 14.5 μm . They are shown in fig. 12. ZrO_2 TBCs have wavelength dependent emissivity⁽⁶⁾, being very small ($\epsilon < 0.4$ or 0.3) at short wavelengths, increasing to almost unity at the longer ($\lambda > 10 \mu\text{m}$) wavelengths. ZrO_2 TBC temperature measurement using the traditional 1- and 2-color pyrometers are known to be difficult. The TBC is flame sprayed on a 25 mm diameter, 6 mm thick metal disk. A 12 mm deep small hole is drilled along a radius 3 mm from the disk surface into which a 250 μm type G thermocouple (TC) is positioned to provide reference temperatures. The disk is placed about 25 mm inside the opening of a black body furnace opening whose temperature is carefully controlled. These spectra (fig. 12) were recorded when the imbedded TC indicated steady readings (at 1110, 1001, 892, 791, 693 and 602 K).

Results In this experiment, the pyrometer is calibrated in the sense that g_λ is known and the measured spectrum is in energy units. The ZrO_2 TBC data of fig. 12 are analyzed according to Eqn 5 assuming $\tau_R=\tau_I=1$, the emissivity ϵ_i is still not known, they will be determined together with the unknown temperature of each spectrum. The 250 μm thick ZrO_2 TBC transmits only less than 1% radiation in a very restricted spectral region (fig. 13), the spectra in fig. 12 must be due to emission or reflection. Reflection is not important in this experiment. λ_R is chosen to be 5 μm and the analysis is done exactly as in case (I) for the unknown transmissivity case. Six spectra were chosen, slopes were determined, an initial value for ϵ_R is chosen, the individual ϵ_i are calculated in terms of ϵ_R and the slopes. The ϵ_i are used to evaluate an average temperature for each spectrum, and similar to case (I), the spectra data are transformed by dividing each spectral datum by ϵ_i , then by $T(t)^5$, the 5th power of the temperature, also the wavelengths are transformed into $c_2/\lambda T(t)$, and the transformed data set (x,y) is least squares curve fitted to the invariant curve. The resultant slope and intercept, emissivity and fitted curve are shown in figs. 14, 15 and 16. The emissivity shown in fig. 15 is very similar to that reported by Liebert⁽⁶⁾. The temperatures were determined to be 1096, 999, 895, 793, 693 and 605 K differing from the TC values by less than 2% (fig. 17).

Conclusion

The multiwavelength pyrometer successfully measured the temperatures of a black body furnace viewed through a transparent window of unknown transmissivity, and also measured the temperature of a zirconia ceramic of unknown emissivity. The measurement error is less than 0.5 % for the first case. This is significant because the pyrometer is not previously calibrated. In the latter case, the error is less than 2 %, this is significant because the measurement is done without prior knowledge of this non-gray (wavelength dependent emissivity) material in the region where the emissivity is inherently small and interference from other sources is always present. By choosing just 2 wavelengths in a good spectral region, temperature determination can be done and is much simplified with a small increase in error.

Reference

1. DeWitt, D.P., Nutter, G.D., Theory and Practice of Radiation Thermometry, John Wiley & Sons, New York, 1988.
2. Hunter, G.B.; Allemand, C; and Eagar, T.W., Multiwavelength Pyrometer - An Improved Method., Opt. Eng., vol. 24, no. 6, Nov.-Dec. 1985, pp. 1081-1085.
3. Ng, Daniel, Williams, W.D., "Full spectrum pyrometry for nongray surface in the presence of interfering radiation", Temperature, Its Measurement and Control in Science and Industry, James F. Schooley Editor, Volume 6, American Institute of Physics, pp 889-894.
4. Ng, Daniel, "A Self-Calibrating, Emissivity Independent Multiwavelength Pyrometer", NASA Conference Publication 10146, 1994, page 28-1 to 28-10.
5. Liebert, C., "Emittance and absorptance of NASA Ceramic Thermal Barrier Coating System", NASA Technical Paper 1190, 1978, Lewis Research Center, Ohio.

Fig. 1
Arrangement of Experiment.

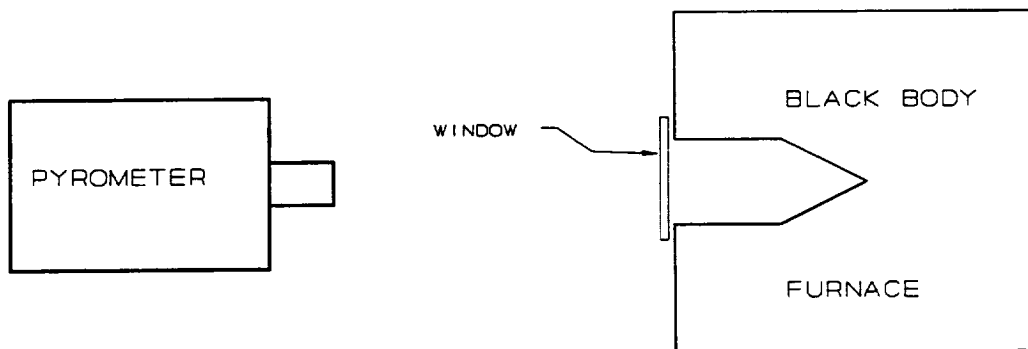


Fig. 2
Voltage spectra of black body furnace viewed through calcium fluoride window.

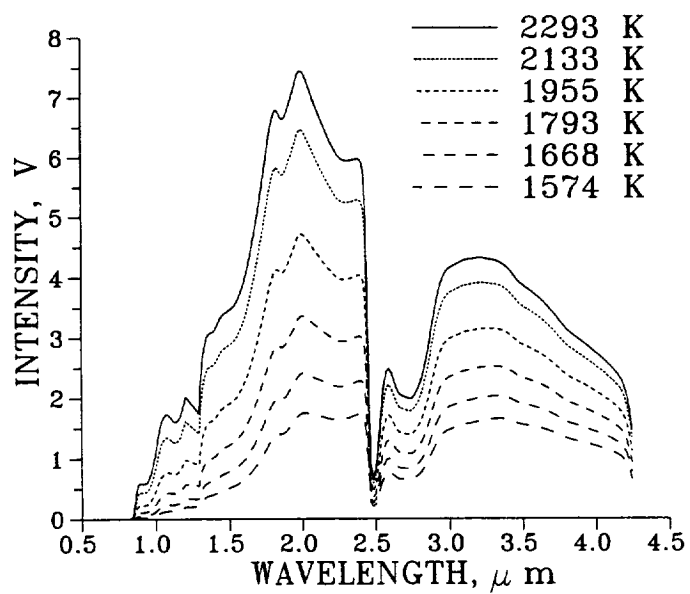


Fig. 3

Plot of data to determine slope and intercept according to Eqn 8, $\lambda_i=1.5 \mu\text{m}$, $\lambda_R=2 \mu\text{m}$.

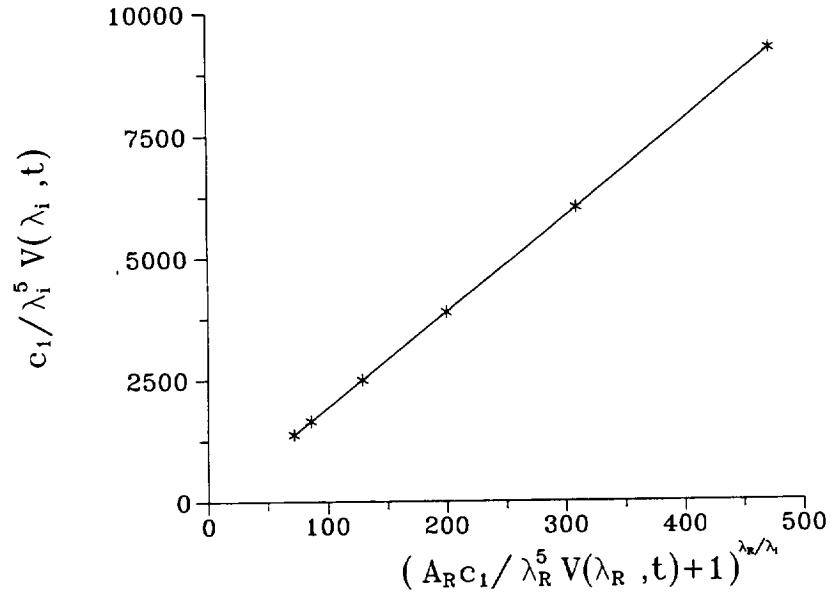


Fig. 4

Slope and intercept results.

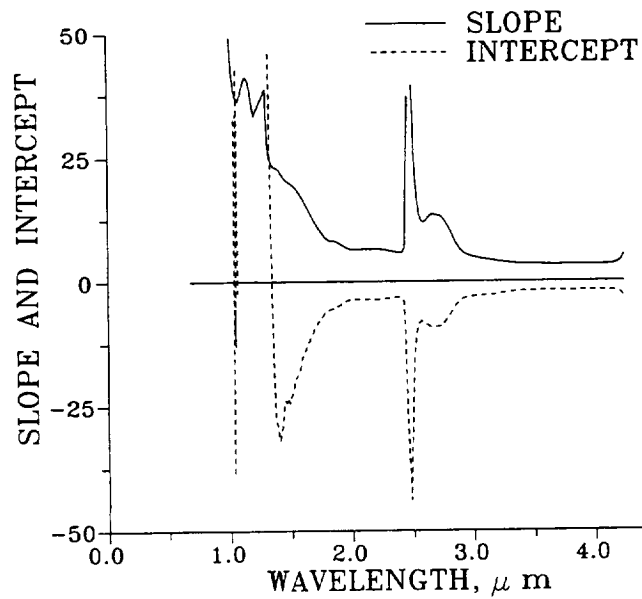


Fig. 5
Calibration constant A_1 as a function of wavelength.

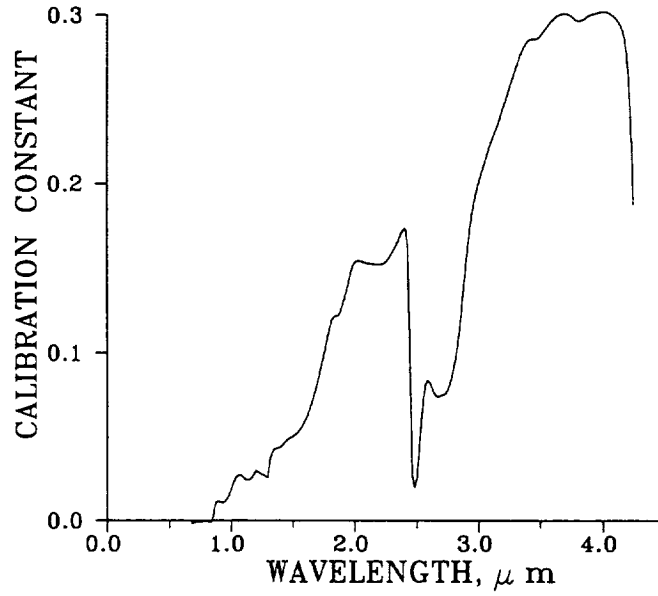


Fig. 6
Temperatures calculated from spectral data and A_1 as a function of wavelength.

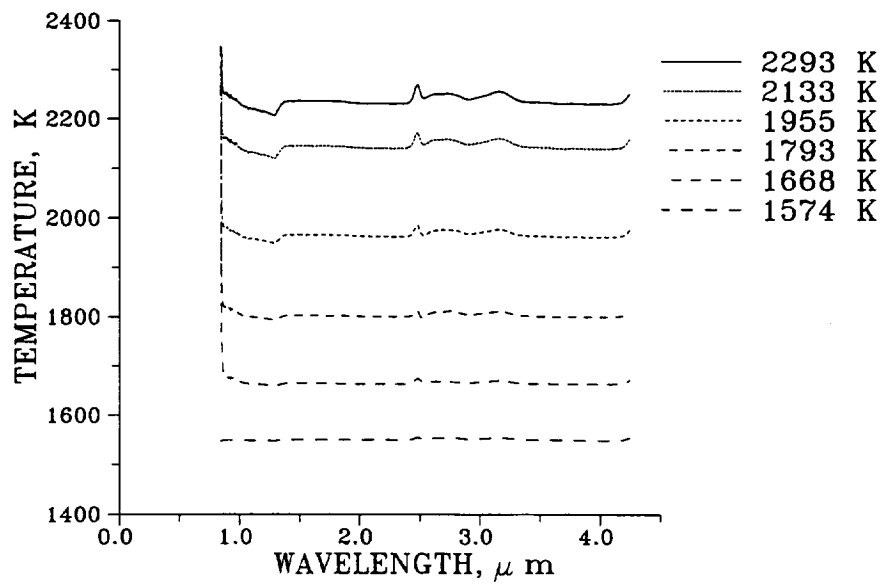


Fig. 7

Least squares curve fitting of the transformed data set to the non-dimensional Planck function.

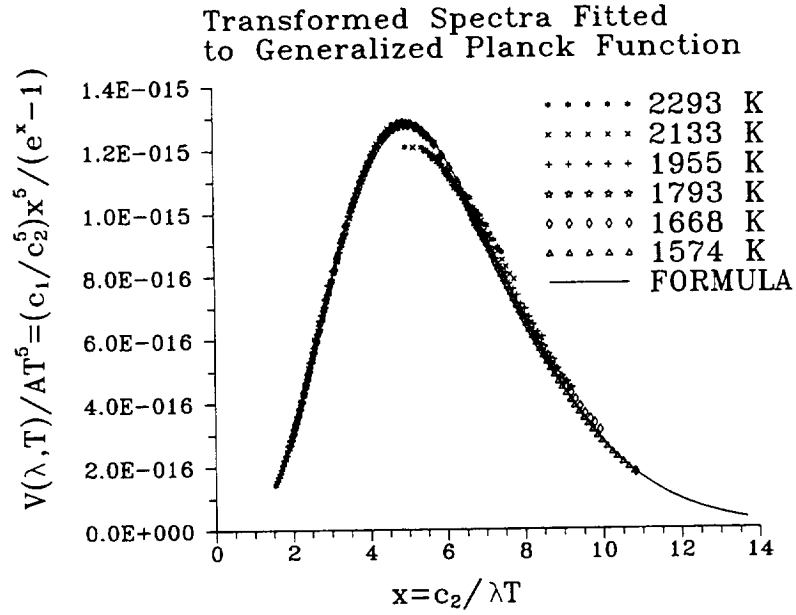


Fig. 8

Plot of pyrometer measured temperature vs black body pre-set temperature.

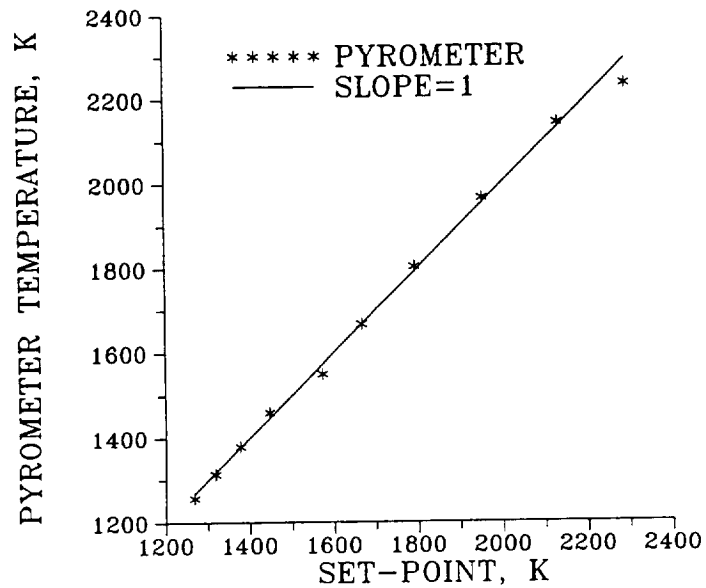


Fig. 9

Least squares curve fitting of the transformed N=2 case data set to the non-dimensional Planck function.

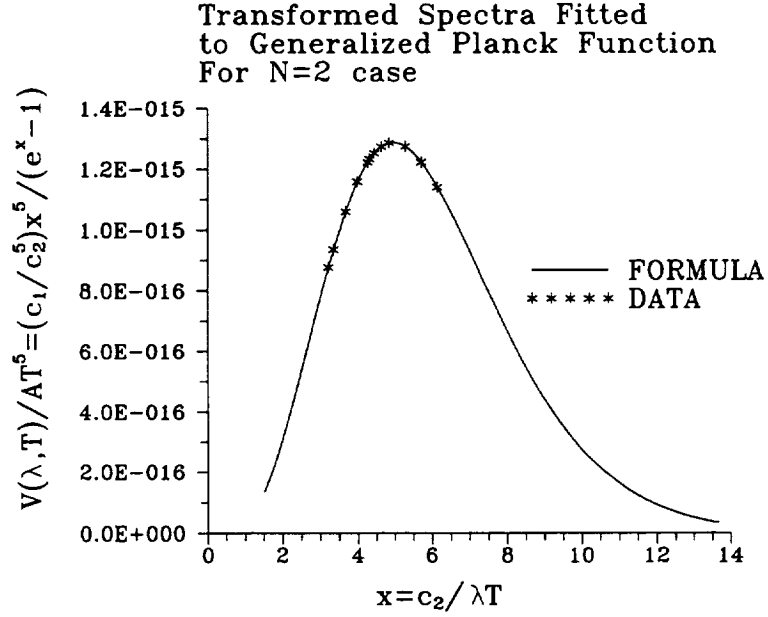
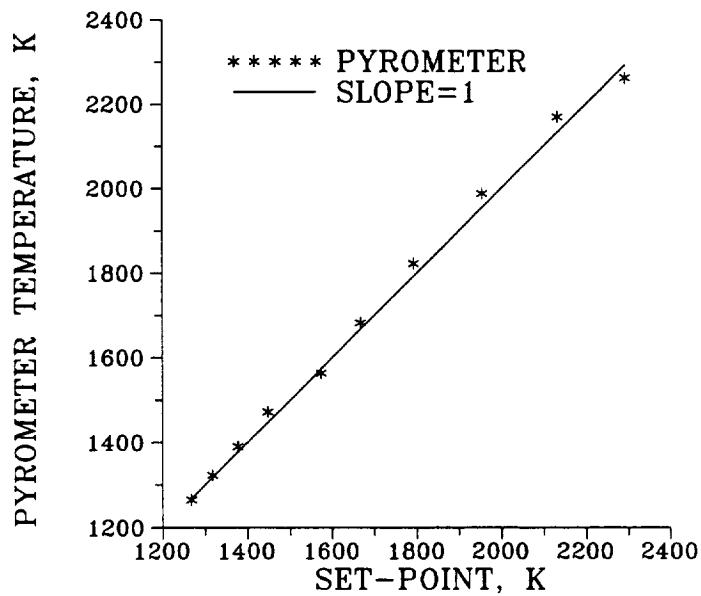


Fig. 10

Plot of pyrometry measured temperature vs black body preset temperature for the N=2 case.



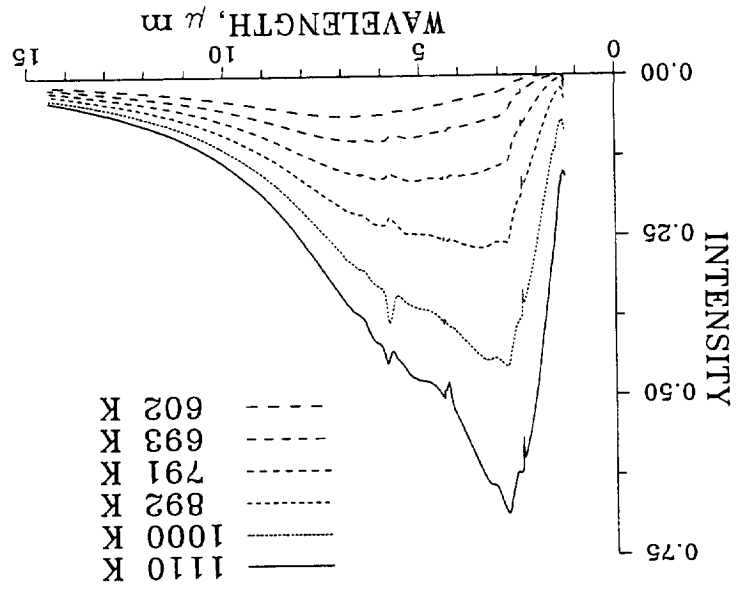


Fig. 12 Spectra of zirconia TBC surface at different temperatures.

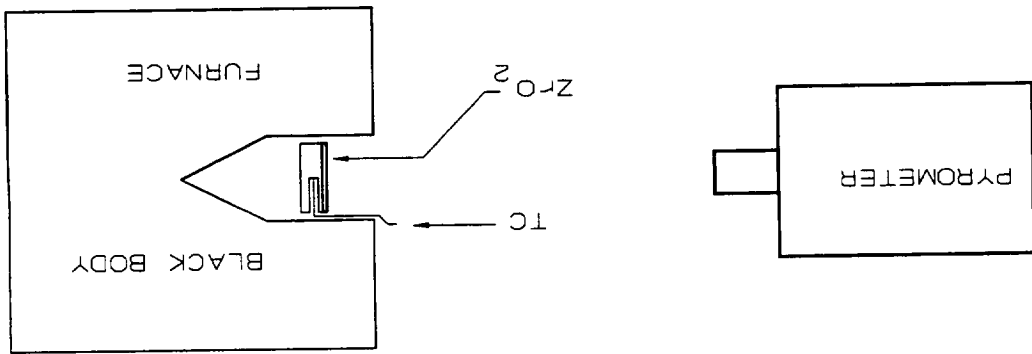


Fig. 11 Arrangement of ZrO₂ experiment.

Fig. 13
Transmission of different thickness zirconia TBCs.

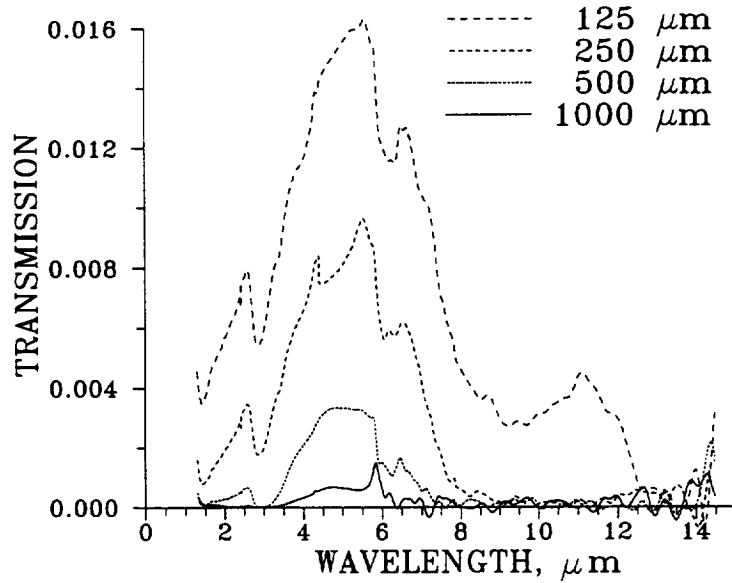


Fig. 14
Slope and intercept results at different wavelengths.

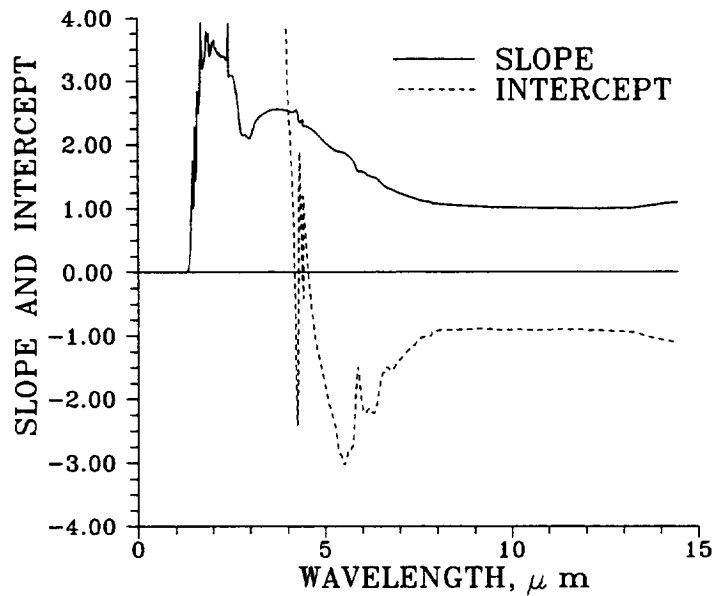


Fig. 15
Emissivity of zirconia TBC as a function of λ , $\epsilon_r=0.5$.

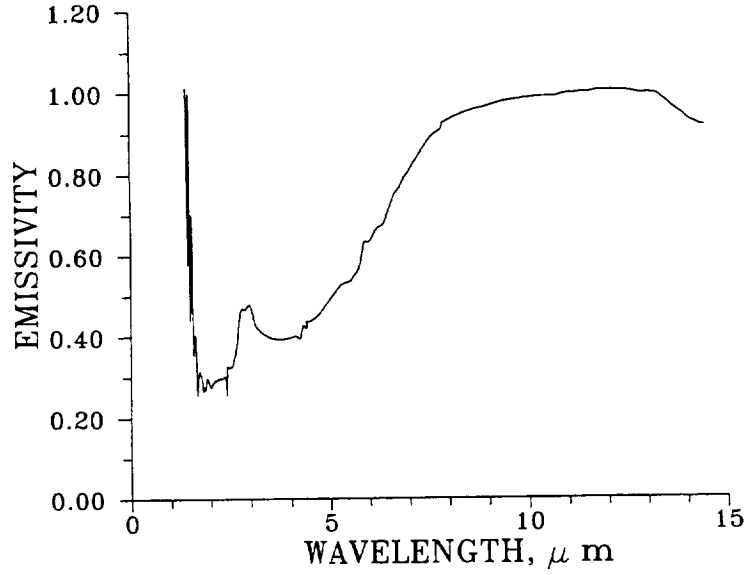


Fig. 16
 ZrO_2 TBC spectra transformed into generalized Planck equation.

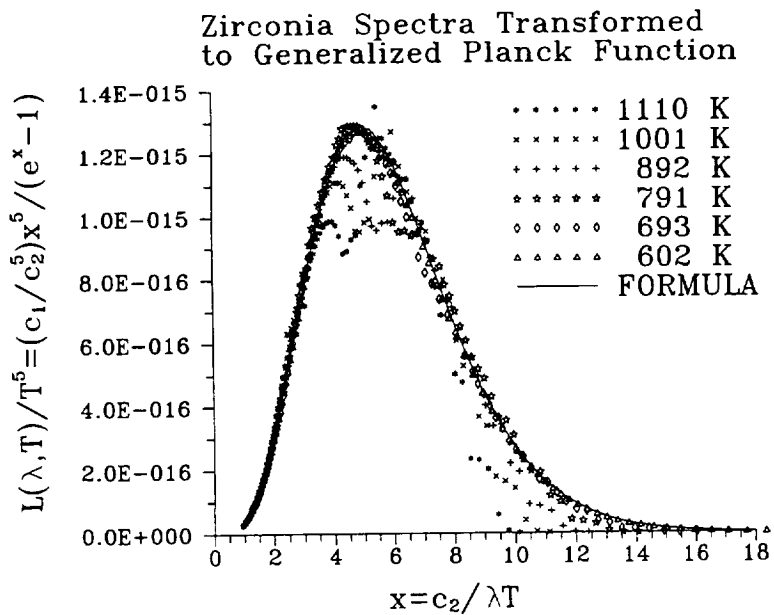
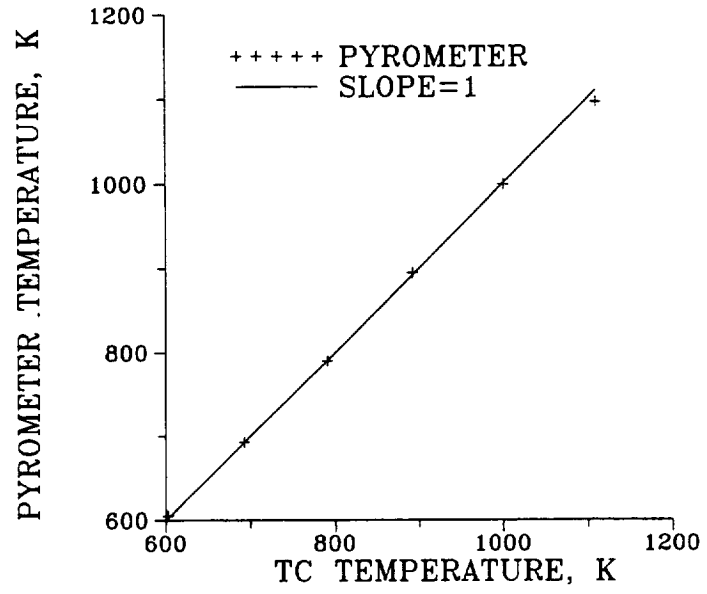


Fig. 17
Pyrometry and thermocouple measured temperatures.



REPORT DOCUMENTATION PAGE			Form Approved OMB No. 0704-0188	
Public reporting burden for this collection of information is estimated to average 1 hour per response, including the time for reviewing instructions, searching existing data sources, gathering and maintaining the data needed, and completing and reviewing the collection of information. Send comments regarding this burden estimate or any other aspect of this collection of information, including suggestions for reducing this burden, to Washington Headquarters Services, Directorate for Information Operations and Reports, 1215 Jefferson Davis Highway, Suite 1204, Arlington, VA 22202-4302, and to the Office of Management and Budget, Paperwork Reduction Project (0704-0188), Washington, DC 20503.				
1. AGENCY USE ONLY (Leave blank)	2. REPORT DATE January 1996	3. REPORT TYPE AND DATES COVERED Technical Memorandum		
4. TITLE AND SUBTITLE A Self Calibrating Emissivity and/or Transmissivity Independent Multiwavelength Pyrometer			5. FUNDING NUMBERS WU-505-62-50	
6. AUTHOR(S) Daniel Ng				
7. PERFORMING ORGANIZATION NAME(S) AND ADDRESS(ES) National Aeronautics and Space Administration Lewis Research Center Cleveland, Ohio 44135-3191			8. PERFORMING ORGANIZATION REPORT NUMBER E-10087	
9. SPONSORING/MONITORING AGENCY NAME(S) AND ADDRESS(ES) National Aeronautics and Space Administration Washington, D.C. 20546-0001			10. SPONSORING/MONITORING AGENCY REPORT NUMBER NASA TM-107149	
11. SUPPLEMENTARY NOTES Responsible person, Daniel Ng, organization code 2510, (216) 433-3638.				
12a. DISTRIBUTION/AVAILABILITY STATEMENT Unclassified - Unlimited Subject Category 35 This publication is available from the NASA Center for Aerospace Information, (301) 621-0390.			12b. DISTRIBUTION CODE	
13. ABSTRACT (Maximum 200 words) Pyrometer is a favorite method to do remote temperature measurement in research and development. One-color, two-color and the disappearing filament pyrometers are most common, multicolor and multiwavelength pyrometers are being introduced recently. All these pyrometers invariably require, in one form or another, information concerning emissivity, the medium transmissivity, their ratio at some two spectral regions, the instrument's calibration constant, etc. for their operation. This information can come from hand books, from the manufacturer or in some instances, from results of dedicated separate experiments. Often this information is sample or instrument specific. Sometimes this information, though obtained from a special experiment, is obtained using a separate sample rather than the one pursued for temperature measurement. Then, there would be the question of variability from sample to sample and variability from batch to batch in the sample used. Also, previously determined calibrations can change with time, and the only way to reduce uncertainty is to perform the calibration more frequently or even immediately before the experiment. We have developed a multiwavelength pyrometer, which eliminates the need to supply the necessary emissivity and/or transmissivity information and the instrument calibration constants ahead of time. The pyrometer calibrates itself from its first cycle data.				
14. SUBJECT TERMS Pyrometry; Emissivity; Zirconia; Temperature			15. NUMBER OF PAGES 16	
			16. PRICE CODE A03	
17. SECURITY CLASSIFICATION OF REPORT Unclassified	18. SECURITY CLASSIFICATION OF THIS PAGE Unclassified	19. SECURITY CLASSIFICATION OF ABSTRACT Unclassified	20. LIMITATION OF ABSTRACT	

**National Aeronautics and
Space Administration**
Lewis Research Center
21000 Brookpark Rd.
Cleveland, OH 44135-3191

Official Business
Penalty for Private Use \$300

POSTMASTER: If Undeliverable — Do Not Return